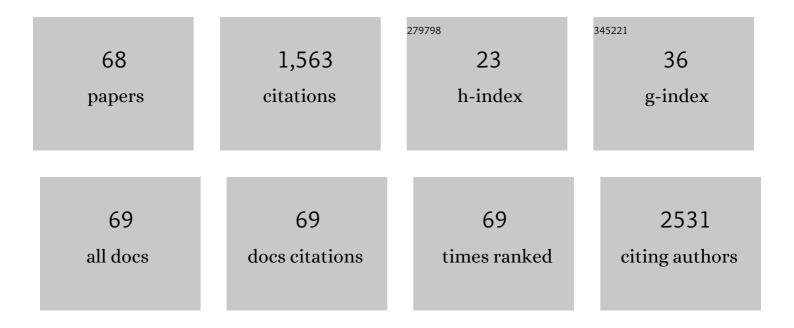
List of Publications by Year in descending order

Source: https://exaly.com/author-pdf/5033366/publications.pdf Version: 2024-02-01



IIDI HENVCH

#	Article	IF	CITATIONS
1	Strongly luminescent monolayered MoS2 prepared by effective ultrasound exfoliation. Nanoscale, 2013, 5, 3387.	5.6	231
2	Chemical mechanical glass polishing with cerium oxide: Effect of selected physico-chemical characteristics on polishing efficiency. Wear, 2016, 362-363, 114-120.	3.1	71
3	Blue and green luminescence of reduced graphene oxide quantum dots. Carbon, 2013, 63, 537-546.	10.3	66
4	Ultrasound exfoliation of inorganic analogues of graphene. Nanoscale Research Letters, 2014, 9, 167.	5.7	58
5	Effect of preparation procedure on the formation of nanostructured ceria–zirconia mixed oxide catalysts for ethyl acetate oxidation: Homogeneous precipitation with urea vs template-assisted hydrothermal synthesis. Applied Catalysis A: General, 2015, 502, 418-432.	4.3	56
6	Magnetically separable reactive sorbent based on the CeO2/Î ³ -Fe2O3 composite and its utilization for rapid degradation of the organophosphate pesticide parathion methyl and certain nerve agents. Chemical Engineering Journal, 2015, 262, 747-755.	12.7	55
7	Cerium oxide for the destruction of chemical warfare agents: A comparison of synthetic routes. Journal of Hazardous Materials, 2016, 304, 259-268.	12.4	54
8	Shape-controlled synthesis of Sn-doped CuO nanoparticles for catalytic degradation of Rhodamine B. Journal of Colloid and Interface Science, 2016, 481, 28-38.	9.4	45
9	Self-Assembled BN and BCN Quantum Dots Obtained from High Intensity Ultrasound Exfoliated Nanosheets. Science of Advanced Materials, 2014, 6, 1106-1116.	0.7	42
10	Degradation of organophosphorus pesticide parathion methyl on nanostructured titania-iron mixed oxides. Applied Surface Science, 2015, 344, 9-16.	6.1	35
11	Nanocrystalline cerium oxide prepared from a carbonate precursor and its ability to breakdown biologically relevant organophosphates. Environmental Science: Nano, 2017, 4, 1283-1293.	4.3	34
12	Reactive adsorption and photodegradation of soman and dimethyl methylphosphonate on TiO2/nanodiamond composites. Applied Catalysis B: Environmental, 2019, 259, 118097.	20.2	32
13	Doping of <scp> <scp>TiO</scp> </scp> ₂ â€" <scp> <scp>GO</scp> </scp> and <scp> <scp>TiO</scp> </scp> ₂ â€"r <scp> GO</scp> with Noble Metals: Synthesis, Characterization and Photocatalytic Performance for Azo Dye Discoloration. Photochemistry and Photobiology, 2013, 89, 1038-1046.	2.5	31
14	Mesoporous manganese oxide for the degradation of organophosphates pesticides. Journal of Materials Science, 2016, 51, 2634-2642.	3.7	31
15	h-BN-TiO ₂ Nanocomposite for Photocatalytic Applications. Journal of Nanomaterials, 2016, 2016, 1-12.	2.7	28
16	Accelerated dephosphorylation of adenosine phosphates and related compounds in the presence of nanocrystalline cerium oxide. Environmental Science: Nano, 2016, 3, 847-856.	4.3	28
17	Reactive adsorption of toxic organophosphates parathion methyl and DMMP on nanostructured Ti/Ce oxides and their composites. Arabian Journal of Chemistry, 2019, 12, 4258-4269.	4.9	28
18	Photocatalytic degradation of ciprofloxacin in water at nano-ZnO prepared by pulse alternating current electrochemical synthesis. Journal of Water Process Engineering, 2021, 40, 101809.	5.6	28

#	Article	IF	CITATIONS
19	Hydrogen peroxide route to Sn-doped titania photocatalysts. Chemistry Central Journal, 2012, 6, 113.	2.6	27
20	Enhanced visible-light photodegradation of fluoroquinolone-based antibiotics and <i>E. coli</i> growth inhibition using Ag–TiO ₂ nanoparticles. RSC Advances, 2021, 11, 13980-13991.	3.6	26
21	Graphene oxide/MnO 2 nanocomposite as destructive adsorbent of nerve-agent simulants in aqueous media. Applied Surface Science, 2017, 412, 19-28.	6.1	25
22	Can cerium oxide serve as a phosphodiesterase-mimetic nanozyme?. Environmental Science: Nano, 2019, 6, 3684-3698.	4.3	25
23	Size Effects on Surface Chemistry and Raman Spectra of Sub-5 nm Oxidized High-Pressure High-Temperature and Detonation Nanodiamonds. Journal of Physical Chemistry C, 2021, 125, 5647-5669.	3.1	25
24	Recovery of Cerium Dioxide from Spent Glass-Polishing Slurry and Its Utilization as a Reactive Sorbent for Fast Degradation of Toxic Organophosphates. Advances in Materials Science and Engineering, 2015, 2015, 1-8.	1.8	24
25	A green method of graphene preparation in an alkaline environment. Ultrasonics Sonochemistry, 2015, 24, 65-71.	8.2	24
26	Chemical warfare agent simulant DMMP reactive adsorption on TiO2/graphene oxide composites prepared via titanium peroxo-complex or urea precipitation. Journal of Hazardous Materials, 2018, 359, 482-490.	12.4	23
27	Bifunctional TiO2/CeO2 reactive adsorbent/photocatalyst for degradation of bis-p-nitrophenyl phosphate and CWAs. Chemical Engineering Journal, 2021, 414, 128822.	12.7	22
28	Template-assisted hydrothermally obtained titania-ceria composites and their application as catalysts in ethyl acetate oxidation and methanol decomposition with a potential for sustainable environment protection. Applied Surface Science, 2017, 396, 1289-1302.	6.1	19
29	ZnO/Bi2O3 nanowire composites as a new family of photocatalysts. Powder Technology, 2015, 270, 83-91.	4.2	18
30	Graphene oxide and graphitic carbon nitride nanocomposites assembled by electrostatic attraction forces: Synthesis and characterization. Materials Chemistry and Physics, 2019, 228, 228-236.	4.0	18
31	Mesoporous cerium oxide for fast degradation of aryl organophosphate flame retardant triphenyl phosphate. RSC Advances, 2019, 9, 32058-32065.	3.6	17
32	Size and nitrogen inhomogeneity in detonation and laser synthesized primary nanodiamond particles revealed via salt-assisted deaggregation. Carbon, 2021, 171, 230-239.	10.3	17
33	Room-temperature synthesis of nanoceria for degradation of organophosphate pesticides and its regeneration and reuse. RSC Advances, 2020, 10, 14441-14450.	3.6	16
34	Nanocrystalline cerium oxide for catalytic degradation of paraoxon methyl: Influence of CeO2 surface properties. Journal of Environmental Chemical Engineering, 2021, 9, 106229.	6.7	15
35	Water-based synthesis of TiO2/CeO2 composites supported on plasma-treated montmorillonite for parathion methyl degradation. Applied Clay Science, 2017, 144, 26-35.	5.2	14
36	Design and Performance of Novel Self-Cleaning g-C3N4/PMMA/PUR Membranes. Polymers, 2020, 12, 850.	4.5	14

#	Article	IF	CITATIONS
37	Feasible Synthesis of TiO ₂ Deposited on Kaolin for Photocatalytic Applications. Clays and Clay Minerals, 2013, 61, 165-176.	1.3	13
38	Photocatalytic and electrochemical properties of single- and multi-layer sub-stoichiometric titanium oxide coatings prepared by atmospheric plasma spraying. Journal of Advanced Ceramics, 2016, 5, 126-136.	17.4	13
39	Template-assisted hydrothermally synthesized iron-titanium binary oxides and their application as catalysts for ethyl acetate oxidation. Applied Catalysis A: General, 2016, 528, 24-35.	4.3	13
40	Solar light decomposition of warfare agent simulant DMMP on TiO2/graphene oxide nanocomposites. Catalysis Science and Technology, 2019, 9, 1816-1824.	4.1	13
41	Mesoporous TiO2 powders as host matrices for iron nanoparticles. Effect of the preparation procedure and doping with Hf. Nano Structures Nano Objects, 2016, 7, 56-63.	3.5	12
42	Iron modified titanium–hafnium binary oxides as catalysts in total oxidation of ethyl acetate. Catalysis Communications, 2016, 81, 14-19.	3.3	12
43	Role of bismuth in nano-structured doped TiO2 photocatalyst prepared by environmentally benign soft synthesis. Journal of Materials Science, 2014, 49, 3560-3571.	3.7	11
44	Chemical degradation of trimethyl phosphate as surrogate for organo-phosporus pesticides on nanostructured metal oxides. Materials Research Bulletin, 2015, 61, 259-269.	5.2	11
45	Formation of Catalytic Active Sites in Hydrothermally Obtained Binary Ceria–Iron Oxides: Composition and Preparation Effects. ACS Applied Materials & Interfaces, 2021, 13, 1838-1852.	8.0	11
46	Nanostructured manganese oxides as highly active catalysts for enhanced hydrolysis of bis(4-nitrophenyl)phosphate and catalytic decomposition of methanol. Catalysis Science and Technology, 2021, 11, 1766-1779.	4.1	11
47	Nanostructured Metal Oxides for Stoichiometric Degradation of Chemical Warfare Agents. Reviews of Environmental Contamination and Toxicology, 2016, 236, 239-258.	1.3	10
48	Synthesis and characterization of TiO ₂ /Mg(OH) ₂ composites for catalytic degradation of CWA surrogates. RSC Advances, 2020, 10, 19542-19552.	3.6	10
49	Graphene oxide nanoparticle attachment and its toxicity on living lung epithelial cells. RSC Advances, 2015, 5, 59447-59457.	3.6	9
50	Novel synthesis of Ag@AgCl/ZnO by different radiation sources including radioactive isotope 60Co: Physicochemical and antimicrobial study. Applied Surface Science, 2020, 529, 147098.	6.1	9
51	Impact of Ge ⁴⁺ Ion as Structural Dopant of Ti ⁴⁺ in Anatase: Crystallographic Translation, Photocatalytic Behavior, and Efficiency under UV and VIS Irradiation. Journal of Nanomaterials, 2012, 2012, 1-11.	2.7	8
52	Mesoporous copper-ceria-titania ternary oxides as catalysts for environmental protection: Impact of Ce/Ti ratio and preparation procedure. Applied Catalysis A: General, 2020, 595, 117487.	4.3	8
53	Photocatalytic oxidation of butane by titania after reductive annealing. Journal of Materials Science, 2014, 49, 4161-4170.	3.7	6
54	<i>In Situ </i> <scp>FTIR</scp> Spectroscopy Study of the Photodegradation of Acetaldehyde and azo Dye Photobleaching on Bismuthâ€Modified TiO ₂ . Photochemistry and Photobiology, 2015, 91, 48-58.	2.5	6

#	Article	IF	CITATIONS
55	Titania and zirconia binary oxides as catalysts for total oxidation of ethyl acetate and methanol decomposition. Journal of Environmental Chemical Engineering, 2018, 6, 2540-2550.	6.7	6
56	Structure and catalytic activity of hydrothermally obtained titanium-tin binary oxides for sustainable environment: Evaluation and control. Microporous and Mesoporous Materials, 2019, 276, 223-231.	4.4	6
5 7	Crucial cytotoxic and antimicrobial activity changes driven by amount of doped silver in biocompatible carbon nitride nanosheets. Colloids and Surfaces B: Biointerfaces, 2021, 202, 111680.	5.0	6
58	Effect of crystal structure on nanofiber morphology and chemical modification; design of CeO2/PVDF membrane. Polymer Testing, 2022, 110, 107568.	4.8	6
59	Graphene Oxide Normal (GO + Mn2+) and Ultrapure: Short-Term Impact on Selected Antioxidant Stress Markers and Cytokines in NHDF and A549 Cell Lines. Antioxidants, 2021, 10, 765.	5.1	5
60	Anthropogenic records in a fluvial depositional system: The Odra River along The Czech-Polish border. Anthropocene, 2021, 34, 100286.	3.3	5
61	Nickel-Decorated Mesoporous Iron–Cerium Mixed Oxides: Microstructure and Catalytic Activity in Methanol Decomposition. ACS Applied Materials & Interfaces, 2022, 14, 873-890.	8.0	5
62	Fast and Straightforward Synthesis of Luminescent Titanium(IV) Dioxide Quantum Dots. Journal of Nanomaterials, 2017, 2017, 1-9.	2.7	3
63	Laser-Induced Modification of Hydrogenated Detonation Nanodiamonds in Ethanol. Nanomaterials, 2021, 11, 2251.	4.1	3
64	Design Control of Copper-Doped Titania–Zirconia Catalysts for Methanol Decomposition and Total Oxidation of Ethyl Acetate. Symmetry, 2022, 14, 751.	2.2	3
65	Degradation of parathion methyl by reactive sorption on the cerium oxide surface: The effect of solvent on the degradation efficiency. Arabian Journal of Chemistry, 2022, 15, 103852.	4.9	3
66	Improvement of Orange II Photobleaching by Moderate Ga3+Doping of Titania and Detrimental Effect of Structural Disorder on Ga Overloading. Journal of Nanomaterials, 2014, 2014, 1-11.	2.7	2
67	Multi-component titanium–copper–cobalt- and niobium nanostructured oxides as catalysts for ethyl acetate oxidation. Reaction Kinetics, Mechanisms and Catalysis, 2015, 116, 397-408.	1.7	1
68	Amidoxime-functionalized bead cellulose for the decomposition of highly toxic organophosphates. RSC Advances, 2021, 11, 17976-17984.	3.6	1